

AD-A127 245

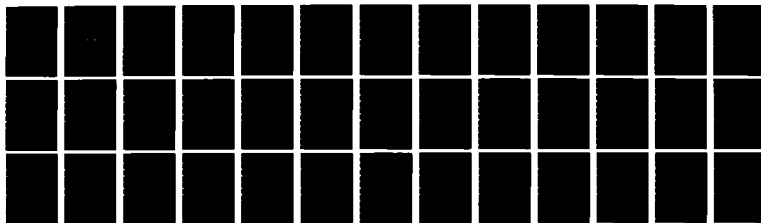
ADAPTIVE ARRAY BEHAVIOR WITH PERIODIC ENVELOPE  
MODULATED INTERFERENCE(U) OHIO STATE UNIV COLUMBUS  
ELECTROSCIENCE LAB A S AL-ROUAIIS ET AL. DEC 82  
ESL-714585-1 N00019-82-C-0198

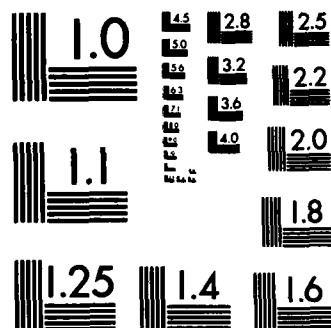
1/1

UNCLASSIFIED

F/G 9/5

NL





MICROCOPY RESOLUTION TEST CHART  
NATIONAL BUREAU OF STANDARDS-1963-A



The Ohio State University

ADAPTIVE ARRAY BEHAVIOR WITH PERIODIC ENVELOPE  
MODULATED INTERFERENCE

A.S. Al-Ruwais  
R.T. Compton, Jr.

The Ohio State University  
**ElectroScience Laboratory**

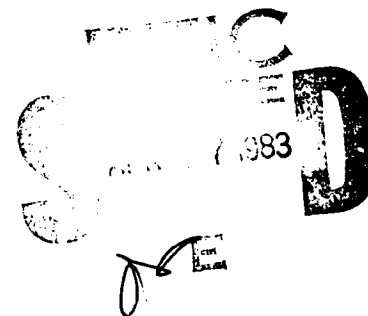
Department of Electrical Engineering  
Columbus, Ohio 43212

Technical Report 714505-1

Contract N00019-82-C-0190

December 1982

Naval Air Systems Command  
Washington, D.C. 20361



APPROVED FOR PUBLIC RELEASE  
DISTRIBUTION UNLIMITED

DTIC FILE COPY

83 04 26 088

## NOTICES

When Government drawings, specifications, or other data are used for any purpose other than in connection with a definitely related Government procurement operation, the United States Government thereby incurs no responsibility nor any obligation whatsoever, and the fact that the Government may have formulated, furnished, or in any way supplied the said drawings, specifications, or other data, is not to be regarded by implication or otherwise as in any manner licensing the holder or any other person or corporation, or conveying any rights or permission to manufacture, use, or sell any patented invention that may in any way be related thereto.

<b>REPORT DOCUMENTATION PAGE</b>		<b>1. REPORT NO.</b> <b>A127245</b>		<b>3. Recipient's Accession No.</b>	
<b>4. Title and Subtitle</b> <b>ADAPTIVE ARRAY BEHAVIOR WITH PERIODIC ENVELOPE MODULATED INTERFERENCE</b>				<b>5. Report Date</b> <b>December 1982</b>	
<b>7. Author(s)</b> <b>A.S. Al-Ruwais and R.T. Compton, Jr.</b>				<b>8. Performing Organization Rept. No.</b> <b>ESL 714505-1</b>	
<b>9. Performing Organization Name and Address</b> <b>The Ohio State University ElectroScience Laboratory Department of Electrical Engineering Columbus, Ohio 43212</b>				<b>10. Project/Task/Work Unit No.</b>	
<b>12. Sponsoring Organization Name and Address</b> <b>Naval Air Systems Command Washington, D.C. 20361</b>				<b>11. Contract(C) or Grant(G) No.</b> (C) (G) <b>N00019-82-C-0190</b>	
<b>13. Type of Report &amp; Period Covered</b> <b>Technical Report</b>				<b>14.</b>	
<b>15. Supplementary Notes</b> <i>The authors (last name, first)</i>					
<b>16. Abstract (Limit: 200 words)</b> <p>We present a method for determining the effects of envelope modulated interference on an LMS adaptive array. The interference is assumed to have periodic envelope modulation with a bandwidth small compared to the carrier frequency. For such interference, the method allows one to calculate the periodic steady-state behavior of the array weights and the resulting array performance.</p> <p>As an example, we compute the effects of an ordinary amplitude modulated (AM) interference signal on the array. It is shown that such interference causes the array to modulate the desired signal envelope but not its phase. With a DPSK desired signal, AM interference is found to have about the same effect on bit error probability as CW interference.</p> <p><i>Completed are</i></p>					
<b>17. Document Analysis a. Descriptors</b>					
<b>b. Identifiers/Open-Ended Terms</b>					
<b>c. COSATI Field/Group</b>					
<b>18. Availability Statement</b> <b>APPROVED FOR PUBLIC RELEASE DISTRIBUTION UNLIMITED</b>			<b>19. Security Class (This Report)</b> <b>Unclassified</b>		<b>21. No of Pages</b> <b>33</b>
			<b>20. Security Class (This Page)</b> <b>Unclassified</b>		<b>22. Price</b>

## TABLE OF CONTENTS

	Page
LIST OF FIGURES	iv
I. INTRODUCTION	1
II. FORMULATION OF THE PROBLEM	3
III. AN EXAMPLE	20
A. <u>Typical Waveforms</u>	22
B. <u>The Effect of Angle of Arrival</u>	25
C. <u>The Effect of Modulation Frequency</u>	25
D. <u>The Effect of Interference-to-Noise Ratio</u>	25
E. <u>The Effect of Desired Signal-to-Noise Ratio</u>	25
F. <u>Bit Error Probability</u>	29
IV. SUMMARY	32
V. REFERENCES	32

<b>Accession For</b>	
NTIS GRA&I	<input checked="" type="checkbox"/>
DTIC TAB	<input type="checkbox"/>
Unannounced	<input type="checkbox"/>
Justification _____	
By _____	
Distribution _____	
Availability Codes	
or	
Dist _____	
<div style="font-size: 2em; font-weight: bold; display: inline-block;">A</div>	



# LIST OF FIGURES

FIGURE	Page
1. <u>A Three-Element LMS Array.</u>	4
2. <u>AM Interference.</u>	7
3. <u><math>A_{dn}(t')</math> versus time.</u> $\theta_d=0^\circ$ , $\theta_i=5^\circ$ , $\epsilon_d=10$ dB. $\epsilon_i=20$ dB, $f'_m=2$ .	23
4. <u>INR versus time.</u> $\theta_d=0^\circ$ , $\theta_i=5^\circ$ , $\epsilon_d=10$ dB. $\epsilon_i=20$ dB, $f'_m=2$ .	23
5. <u>SINR versus time.</u> $\theta_d=0^\circ$ , $\theta_i=5^\circ$ , $\epsilon_d=10$ dB. $\epsilon_i=20$ dB, $f'_m=2$ .	23
6. <u><math>m</math> versus <math>\theta_i</math></u> $\theta_d=0^\circ$ , $\epsilon_d=10$ dB, $f'_m=2$ .	26
7. <u><math>a_{max}</math> versus <math>\theta_i</math></u> $\theta_d=0^\circ$ , $\epsilon_d=10$ dB, $f'_m=2$ .	26
8. <u><math>m</math> versus <math>f'_m</math></u> $\theta_d=0^\circ$ , $\epsilon_d=0$ dB, $\epsilon_i=20$ dB.	27
9. <u><math>a_{max}</math> versus <math>f'_m</math></u> $\theta_d=0^\circ$ , $\epsilon_d=0$ dB, $\epsilon_i=20$ dB.	27

## FIGURE

Page

- |     |  |    |
|-----|--|----|
| 10. | $\frac{m \text{ versus } f_m'}{\theta_d=0^\circ, \theta_i=5^\circ, \xi_d=0 \text{ dB.}}$                     | 28 |
| 11. | $\frac{a_{\max} \text{ versus } f_m'}{\theta_d=0^\circ, \theta_i=5^\circ, \xi_d=0 \text{ dB.}}$              | 28 |
| 12. | $\frac{m \text{ versus } f_m'}{\theta_d=0^\circ, \theta_i=5^\circ, \xi_i=20 \text{ dB.}}$                    | 30 |
| 13. | $\frac{a_{\max} \text{ versus } f_m'}{\theta_d=0^\circ, \theta_i=5^\circ, \xi_i=20 \text{ dB.}}$             | 30 |
| 14. | $\frac{\text{Bit error probability versus } f_m'}{\theta_d=0^\circ, \theta_i=30^\circ, \xi_d=6 \text{ dB.}}$ | 31 |



## I. INTRODUCTION

The performance of an LMS (Least Mean Square) adaptive array [1] can be different with modulated interference than with single frequency (CW) interference. Under certain conditions, interference modulated at a rate slow enough to be tracked by the array feedback can cause the weights to vary continuously and prevent them from reaching steady-state. In this situation the output signal-to-interference-plus-noise ratio (SINR) from the array varies continuously and the array modulates the desired signal.

Pulsed interference is a simple example of modulated interference. The effect of a pulsed interference signal on an adaptive array has been described in [2]. It was shown, for example, that when the array receives a differential phase-shift keyed (DPSK) communication signal, pulsed interference increases the bit error probability more than CW interference for certain choices of the signal parameters.

The behavior of an LMS array has also been described for a double-sideband, suppressed carrier, amplitude modulated (DSBSC-AM) interference signal [3]. This special modulation was studied because it results in a differential equation for the array weights that can be solved. (Arbitrary types of interference modulation lead to an intractable mathematical problem.) For DSBSC-AM interference, the array weights satisfy a vector differential equation with properties similar

to the classical Mathieu equation [4]. By using an approach similar to the classical technique, it is possible to obtain the complete behavior of the array weights for this type of interference. It was shown in [3] that DSBSC-AM interference can cause the array to modulate the desired signal envelope, but that its effect on bit error probability with a DPSK signal is not much different than that of CW interference.

The purpose of the present report is to extend the technique used in [3] to handle interference with more general types of envelope modulation. The technique we present here requires that the interference have only envelope modulation (i.e., no phase modulation) and that the interference modulation be periodic. Also, it must be possible to approximate the interference modulation with a finite number of Fourier Series terms. In principle the number of terms used can be any finite number, but in practice the computational effort increases with the number of terms.

To illustrate the use of this method, we examine the LMS array performance with a simple amplitude modulated (AM) interference signal (a carrier and two sidebands). In general, this interference has the same effects on array performance as pulsed and DSBSC-AM interference: it causes the array output SINR to vary with time, and it produces envelope modulation, but not phase modulation, on the desired signal.

Section II of the report presents a method that can be used to determine the array weights and evaluate the array performance for an interference signal with arbitrary periodic envelope modulation. Section III presents calculated results obtained with this method for an AM interference signal. Section IV contains the conclusions.

## II. FORMULATION OF THE PROBLEM

Consider an adaptive array with three isotropic elements a half wavelength apart, as shown in Figure 1. The analytic signal  $\tilde{x}_j(t)$  from element  $j$  is multiplied by complex weight  $w_j$  and summed to produce the array output  $\tilde{s}(t)$ . The error signal  $\tilde{e}(t)$  is the difference between the reference signal  $\tilde{r}(t)$  and the array output  $\tilde{s}(t)$ . The array weights are controlled by LMS feedback loops [1,5] and satisfy the system of equations

$$\frac{dW}{dt} + k\phi W = kS \quad (1)$$

where  $W = (w_1, w_2, w_3)^T$  is the weight vector,  $\phi$  is the covariance matrix,

$$\phi = E(X^* X^T) \quad (2)$$

$S$  is the reference correlation vector,

$$S = E[X^* \tilde{r}(t)], \quad (3)$$

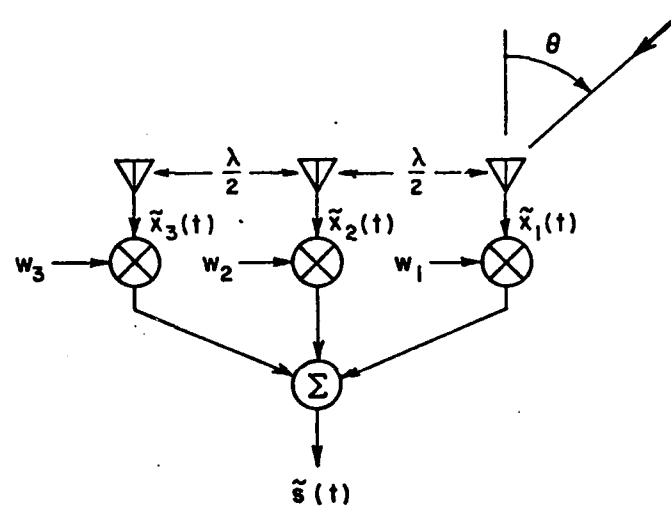


Figure 1. A Three-Element LMS Array.

and  $k$  is the LMS loop gain. In these equations,  $X$  is the signal vector,

$$X = [\tilde{x}_1(t), \tilde{x}_2(t), \tilde{x}_3(t)]^T, \quad (4)$$

$T$  denotes transpose,  $*$  complex conjugate, and  $E[\cdot]$  expectation.

We assume that a desired and an interference signal are incident on the array and that thermal noise is also present in each element signal. The signal vector then contains three terms,

$$X = X_d + X_i + X_n, \quad (5)$$

where  $X_d$ ,  $X_i$  and  $X_n$  are the desired, interference and thermal noise vectors, respectively.

We assume the desired signal is CW and incident from angle  $\theta_d$  relative to broadside. ( $\theta$  is defined in Figure 1.) The desired signal vector is then

$$X_d = A_d e^{j(\omega_0 t + \psi_d)} U_d, \quad (6)$$

where  $A_d$  is the amplitude,  $\omega_0$  is the carrier frequency,  $\psi_d$  is the carrier phase angle, and  $U_d$  is a vector containing the interelement phase shifts,

$$U_d = (1, e^{-j\phi_d}, e^{-j2\phi_d})^T, \quad (7)$$

with

$$\phi_d = \pi \sin \theta_d. \quad (8)$$

We assume  $\psi_d$  is a random variable uniformly distributed on  $(0, 2\pi)$ .

Next, we assume an envelope modulated interference signal, as shown in Figure 2, arriving from angle  $\theta_i$ . The interference signal vector is

$$X_i = A_i e^{j(\omega_0 t + \psi_i)} \begin{pmatrix} a_i(t) \\ a_i(t - T_i) e^{-j\omega_0 T_i} \\ a_i(t - 2T_i) e^{-j2\omega_0 T_i} \end{pmatrix} \quad (9)$$

where  $A_i$  is the amplitude,  $a_i(t)$  is the envelope modulation received on element 1,  $\psi_i$  is the carrier phase angle, and  $T_i$  is the interelement time delay,

$$T_i = \frac{\pi}{\omega_0} \sin \theta_i \quad (10)$$

We assume  $\psi_i$  is a random variable uniformly distributed on  $(0, 2\pi)$  and statistically independent of  $\psi_d$ .

We assume the modulation envelope  $a_i(t)$  is a periodic waveform. To make the definitions of  $a_i(t)$  and  $A_i$  unique, we assume  $a_i(t)$  has a peak value of unity during the period:

$$\begin{aligned} \max a_i(t) &= 1 \\ 0 &\leq t < T \end{aligned} \quad (11)$$

where  $T$  is the period of  $a_i(t)$ . With this normalization,  $A_i^2$  is the peak interference power per array element. In addition, we assume the rate

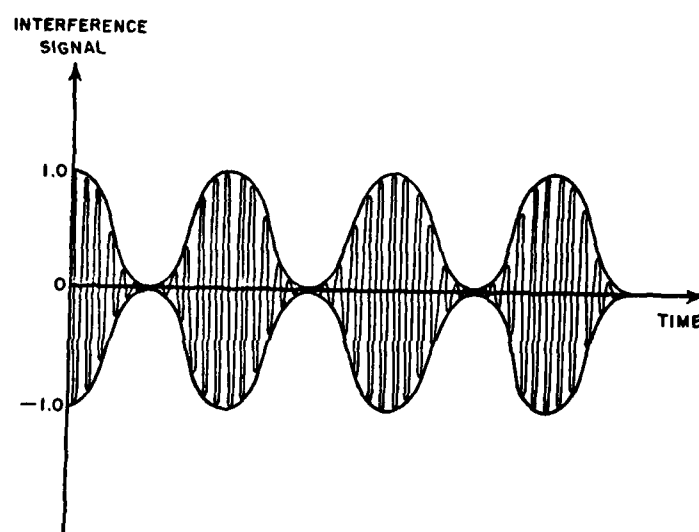


Figure 2. AM Interference.

of change of  $a_i(t)$  is small enough that  $a_i(t)$  changes only a negligible amount during the propagation time  $2T_i$  across the array. (Or, equivalently, we assume that the bandwidth of  $a_i(t)$  is very small compared to the carrier frequency  $\omega_0$ .) Under this condition, the modulation envelopes in (9) are all essentially the same,

$$a_i(t) \approx a_i(t-T_i) \approx a_i(t-2T_i) \quad (12)$$

so (9) may be written

$$x_i = A_i a_i(t) e^{j(\omega_0 t + \psi_i)} u_i \quad (13)$$

where

$$u_i = (1, e^{-j\phi_i}, e^{-j2\phi_i}) \quad (14)$$

with

$$\phi_i = \omega_0 T_i = \pi \sin \theta_i \quad (15)$$

Finally, we assume the thermal noise vector is given by

$$x_n = [\tilde{n}_1(t), \tilde{n}_2(t), \tilde{n}_3(t)]^T, \quad (16)$$

where the  $\tilde{n}_j(t)$  are zero-mean, gaussian thermal noise voltages, all statistically independent of each other and of  $\psi_d$  and  $\psi_i$ , and each of power  $\sigma^2$ . Thus,

$$E[\tilde{n}_j^*(t) \tilde{n}_k(t)] = \sigma^2 \delta_{jk}, \quad (17)$$



Under these assumptions, the covariance matrix in (2) becomes

$$\Phi = \Phi_d + \Phi_i + \Phi_n, \quad (18)$$

with

$$\Phi_d = A_d^2 U_d^* U_d^T \quad (19)$$

$$\Phi_i = A_i^2 a_i^2(t) U_i^* U_i^T \quad (20)$$

and

$$\Phi_n = \sigma^2 I, \quad (21)$$

where  $I$  is the identity matrix.

To compute the reference correlation vector  $S$  in (3), the reference signal  $\tilde{r}(t)$  must first be defined. In practice, the reference signal is usually derived from the array output [6-8]. It must be a signal correlated with the desired signal and uncorrelated with the interference. Here we assume the reference signal to be a replica of the desired signal,

$$\tilde{r}(t) = A_r e^{j(\omega_0 t + \psi_d)}. \quad (22)$$

Equation (3) then yields

$$S = A_r A_d^* U_d^* . \quad (23)$$

Equations (18)-(21) and (23) can now be inserted into (1) to give the differential equation for the weight vector  $W$ ,

$$\frac{dW}{dt} = k[\sigma^2 I + A_d^2 U_d^* U_d^T + A_i^2 a_i^2(t) U_i^* U_i^T] W(t) = k A_r A_d U_d^* \quad (24)$$

Before solving (24) we put it in normalized form. First, dividing by  $k\sigma^2$  gives

$$\frac{dW(t')}{dt'} + [I + \xi_d U_d^* U_d^T + \xi_i a_i^2(t') U_i^* U_i^T] W(t') = \frac{A_r}{\sigma} \sqrt{\xi_d} U_d^* \quad (25)$$

where

$$\xi_d = \frac{A_d^2}{\sigma^2} = \text{input signal-to-noise ratio (SNR) per element.}$$

$$\xi_i = \frac{A_i^2}{\sigma^2} = \text{peak input interference-to-noise ratio (INR) per element,}$$

and where we have also used a normalized time variable,

$$t' = k\sigma^2 t = \text{normalized time.}$$

Next, we note that the constant  $A_r/\sigma$  on the right side of (25) will just appear as a scale factor in the solution for  $W$ . It has no effect on the array output signal-to-noise ratios to be computed below. Hence, we arbitrarily set  $A_r/\sigma=1$  to eliminate it. Finally, by defining

$$\Phi_1 = I + \xi_d U_d^* U_d^T, \quad (26)$$

Equation (25) may be written

$$\frac{dW(t')}{dt'} + [\phi_1 + \epsilon_i a_i^2(t') U_i^* U_i^T] W(t') = \epsilon_d U_d^* . \quad (27)$$

Since we assumed  $a_i(t)$  to be a periodic waveform,  $a_i^2(t')$  is also periodic and may be expanded in a Fourier series:

$$a_i^2(t') = \sum_{\ell=-\infty}^{\infty} p_{\ell} e^{j\ell\omega'_m t'} \quad (28)$$

where the  $p_{\ell}$  are the Fourier coefficients and  $\omega'_m$  is the normalized fundamental frequency of  $a_i(t')$ . ( $\omega'_m$  is equal to  $\omega_m/k\sigma^2$ , where  $\omega_m$  is the fundamental frequency of  $a_i(t)$ .) As discussed above,  $a_i(t)$  is assumed to have a bandwidth small compared with the carrier frequency  $\omega_0$ . In particular, we shall assume that only a finite number of coefficients in (28) are nonzero, i.e., that  $p_{\ell}=0$  for all  $|\ell|>L$ , where  $L$  is some integer. Equation (28) is then

$$a_i^2(t') = \sum_{\ell=-L}^L p_{\ell} e^{j\ell\omega'_m t'} . \quad (29)$$

Equation (27) is a linear vector differential equation with a constant source term on the right but with periodic time-varying coefficients. As has been discussed by D'Angelo [9], the solution for  $W(t')$  will be a periodic function of time after the initial transients have died out. In this report, we do not consider the initial transients. We concentrate on the periodic steady-state solution for

$W(t')$ . Once any initial transients have ended,  $W(t')$  can be represented by a Fourier Series,

$$W(t') = \sum_{n=-\infty}^{\infty} C_n e^{jn\omega_m t'} \quad (30)$$

where  $C_n$  is a vector Fourier coefficient. Substituting (29) and (30) into (27) and collecting terms with the same frequency, we find that the coefficients  $C_n$  must satisfy

$$(jn\omega_m' I + \Phi_1) C_n + \epsilon_1 U_i^* U_i^T \sum_{\ell=-L}^L P_{\ell} C_{n-\ell} = \sqrt{\epsilon_d} U_d^* \delta_{n0}, \quad -\infty < n < \infty \quad (31)$$

This equation may be solved for the  $C_n$  by expressing each  $C_n$  in terms of its components parallel and perpendicular to the vector  $U_i^*$ . To do this, we form a set of three orthonormal basis vectors\*  $e_k$

$$e_j^\dagger e_k = \delta_{jk}, \quad 1 \leq j, k \leq 3, \quad (32)$$

(where  $\dagger$  is conjugate transpose). We let  $e_1$  be a unit vector parallel to  $U_i^*$ :

$$e_1 = \frac{U_i^*}{\sqrt{U_i^T U_i^*}} \quad (33)$$

---

\*The array has 3 elements, so  $W(t')$  and  $C_n$  each have 3 components. Three basis vectors are needed to span the space for  $C_n$ .

We let  $e_2$  be perpendicular to  $e_1$  and lie in the plane defined by  $U_d^*$  and  $U_i^*$ :

$$e_2 = \zeta[U_d^* - \kappa U_i^*] \quad (34)$$

where  $\zeta$  and  $\kappa$  are constants. Enforcing the orthonormality condition (32) yields

$$\kappa = \frac{U_i^T U_d^*}{U_i^T U_i^*} \quad (35)$$

and

$$\zeta = \left( U_d^T U_d^* - \frac{|U_i^T U_d^*|^2}{U_i^T U_i^*} \right)^{-1/2} \quad (36)$$

The third vector  $e_3$  can readily be found from  $e_1$  and  $e_2$  but will not be needed below, so we shall not compute it explicitly.

Each coefficient  $C_n$  may be written in terms of the unit vectors  $e_k$  as

$$C_n = \sum_{k=1}^3 \alpha_{n,k} e_k \quad (37)$$

where the  $\alpha_{n,k}$  are scalar coefficients.  $\alpha_{n,k}$  is the component of  $C_n$  along the unit vector  $e_k$ .

Substituting (37) into (31) and multiplying the result on the left by  $e_p^\dagger$  (for  $p = 1, 2$  or  $3$ ) gives

$$\begin{aligned}
 jn\omega'_m \sum_{k=1}^3 \alpha_{n,k} \delta_{pk} + \sum_{k=1}^3 \alpha_{n,k} f_{pk} \\
 + \xi_i (e_p^\dagger U_i^*) \sum_{\ell=-L}^L p_\ell \sum_{k=1}^3 \alpha_{n-\ell,k} (U_i^T e_k) \\
 = \sqrt{\xi_d} (e_p^\dagger U_d^*) \delta_{no} \quad , \quad (38)
 \end{aligned}$$

where

$$f_{pk} = e_p^\dagger \phi_1 e_k \quad . \quad (39)$$

The values of the  $f_{pk}$  may be found from (26) and (32) - (36). The result is

$$f_{11} = 1 + \xi_d \frac{|U_i^T U_d^*|^2}{U_i^T U_i^*} \quad , \quad (40)$$

$$f_{22} = 1 + \frac{\xi_d}{\zeta^2} \quad , \quad (41)$$

$$f_{12} = f_{21}^* = \frac{\xi_d}{\zeta} \frac{U_i^T U_d^*}{\sqrt{U_i^T U_i^*}} \quad , \quad (42)$$

$$f_{13} = f_{31} = f_{23} = f_{32} = 0 , \quad (43)$$

and

$$f_{33} = 1 . \quad (44)$$

To determine the  $\alpha_{n,k}$ , we proceed as follows. First, since  $e_3^\dagger U_i^* = e_3^\dagger U_d^* = 0$ , applying (38) for  $p = 3$  gives

$$\alpha_{n,3} = 0 , \quad -\infty < n < \infty . \quad (45)$$

Then, since  $e_2^\dagger U_i^* = 0$ , applying (38) for  $p = 2$  and rearranging gives

$$\alpha_{n,2} = \frac{\sqrt{\epsilon_d} (e_2^\dagger U_d^*) \delta_{no} - \alpha_{n,1} f_{21}}{jn\omega_m' + f_{22}} . \quad (46)$$

This equation allows us to calculate the  $\alpha_{n,2}$  from  $\alpha_{n,1}$ . Hence, the problem of determining  $W(t')$  is reduced to the problem of finding the  $\alpha_{n,1}$ .

To obtain the  $\alpha_{n,1}$ , we apply (38) for  $p = 1$  and use (46) to substitute for  $\alpha_{n,2}$ . This process yields the following relation between the  $\alpha_{n,1}$ :

$$h_n \alpha_{n,1} + \sum_{\ell=-L}^L p_\ell \alpha_{n-\ell,1} = C \delta_{n0} \quad (47)$$

where

$$h_n = \frac{(f_{11} + jn\omega_m)(f_{22} + jn\omega_m) - |f_{12}|^2}{\epsilon_i (f_{22} + jn\omega_m) |U_i^*|^2} \quad (48)$$

and

$$C = \frac{\sqrt{\epsilon_d}}{\epsilon_i |U_i^*|^2} \left( e_1^\dagger - \frac{f_{12}}{f_{22}} e_2^\dagger \right) U_d^* \quad (49)$$

Equation (47) holds for each value of  $n$  and is a  $2L+1$  term recursion relation between the  $\alpha_{n,1}$ . If the values of  $\alpha_{n,1}$  were known for  $2L$  successive terms, one could find all the other  $\alpha_{n,1}$  from (47). However, if one starts with an arbitrary initial set of  $2L$  terms, the  $\alpha_{n,1}$  will not converge. Since the solution for  $W(t')$  in (30) must converge, the  $\alpha_{n,1}$  must approach zero as  $n \rightarrow \pm\infty$ . To obtain a solution for  $W(t')$ , we therefore use the following method. We assume that there is some  $N$  such that for all  $|n| > N$ , the  $\alpha_{n,1}$  are essentially zero, i.e., we assume that  $W(t')$  in (30) can be adequately approximated by a finite sum

$$W(t') = \sum_{n=-N}^N C_n e^{jn\omega_m t'} \quad (50)$$



If the  $\alpha_{n,1}$  are zero for  $|n| > N$ , then the recursion relation (47) reduces to the finite system of equations,

$$\begin{bmatrix}
 h_N + P_0 & P_1 & \cdots & P_L & 0 & \cdots & 0 & \cdots & 0 \\
 P_{-1} & h_{N-1} + P_0 & P_1 & \cdots & P_L & \cdots & 0 & \cdots & 0 \\
 \vdots & \vdots & \vdots & \vdots & \vdots & \vdots & \vdots & \vdots & \vdots \\
 0 & \cdots & 0 & P_{-L} & \cdots & P_{-1} & h_0 + P_0 & P_1 \cdots P_L & 0 & \cdots & 0 \\
 \vdots & \vdots & \vdots & \vdots & \vdots & \vdots & \vdots & \vdots & \vdots & \vdots & \vdots \\
 \vdots & \vdots & \vdots & \vdots & \vdots & \vdots & \vdots & \vdots & \vdots & \vdots & \vdots \\
 \vdots & \vdots & \vdots & \vdots & \vdots & \vdots & \vdots & \vdots & \vdots & \vdots & \vdots \\
 \vdots & \vdots & \vdots & \vdots & \vdots & \vdots & \vdots & \vdots & \vdots & \vdots & \vdots \\
 0 & \cdots & 0 & \cdots & 0 & P_{-L} & \cdots & \cdots & P_{-1} & h_{-N} + P_0 & \cdots
 \end{bmatrix}
 \begin{bmatrix}
 \alpha_{N,1} \\
 \alpha_{N-1,1} \\
 \vdots \\
 \vdots \\
 \alpha_{0,1} \\
 \vdots \\
 \vdots \\
 \vdots \\
 \vdots \\
 \alpha_{-N,1}
 \end{bmatrix}
 =
 \begin{bmatrix}
 0 \\
 0 \\
 \vdots \\
 \vdots \\
 C \\
 \vdots \\
 \vdots \\
 \vdots \\
 \vdots \\
 0
 \end{bmatrix}
 \quad (51)$$

The nonzero  $\alpha_{n,1}$  can be found by solving (51) numerically.

For this approach to yield accurate results,  $N$  must in fact be large enough that at least  $2L$  of the  $\alpha_{n,1}$  are essentially zero on each end of the  $\alpha_{n,1}$  vector in (51). If this vector has  $2L$  zeros on each end, the solution obtained from (51) will be the same as the solution of the infinite system in (47). In practice, a suitable value of  $N$  may be determined by increasing  $N$  until the  $\alpha_{n,1}$  vector has  $2L$  terms on each

end that are essentially zero. Experience in specific cases quickly shows how large  $N$  must be. Once the  $\alpha_{n,1}$  are determined, the  $\alpha_{n,2}$  may be found from (46). From  $\alpha_{n,1}$  and  $\alpha_{n,2}$  (and  $\alpha_{n,3}=0$ ), the  $C_n$  may be evaluated from (37) and  $W(t')$  from (30).

The time-varying weights in (30) have two effects on array performance. First, they cause the array to modulate the desired signal. (The array becomes a time-varying, or frequency dispersive, channel [10]). Second, the array output signal-to-interference-plus-noise ratio (SINR) varies periodically with time.

Given a time-varying weight vector  $W(t')$ , the desired signal component of the array output is

$$\tilde{s}_d(t') = A_d W^T(t') U_d e^{j(\omega_0' t' + \psi_d)} \quad , \quad (52)$$

(where  $\omega_0' = \omega_0 / k \sigma^2$ ). To study the modulation on  $\tilde{s}_d(t)$ , we define

$$a_d(t') e^{j\eta_d(t')} = A_d W^T(t') U_d \quad . \quad (53)$$

Then  $a_d(t') = A_d |W^T(t') U_d|$  is the envelope modulation and  $\eta_d(t') = \angle W^T(t') U_d$  is the phase modulation. Furthermore, we define  $a_{dn}(t')$  to be the envelope normalized to its value in the absence of interference, i.e.,

$$a_{dn}(t') = \frac{a_d(t')}{A_d |W_0^T U_d|} , \quad (54)$$

where  $W_0$  is the steady-state weight vector that would occur without interference,

$$W_0 = (\Phi_d + \Phi_n)^{-1} S. \quad (55)$$

( $\Phi_d$ ,  $\Phi_n$  and  $S$  are given in (19), (21) and (23).) The results below are presented in terms of  $a_{dn}(t')$  rather than  $a_d(t')$  because the effect of the interference can be seen by comparing  $a_{dn}(t')$  with unity.

The output desired signal power is

$$P_d(t') = (1/2)E\{|\tilde{s}_d(t')|^2\} = (1/2)A_d^2 |W^T(t') U_d|^2 . \quad (56)$$

The output interference signal is

$$\tilde{s}_i(t') = W^T(t') X_i = A_i a_i(t) W^T(t') U_i e^{j(\omega_0 t + \psi_i)} \quad (57)$$

and the output interference power is

$$P_i(t') = (1/2)E\{|\tilde{s}_i(t')|^2\} = (1/2)A_i^2 a_i^2(t) |W^T(t') U_i|^2 . \quad (58)$$

The output thermal noise power is

$$P_n(t') = \frac{\sigma^2}{2} W^\dagger(t') W(t'). \quad (59)$$

From these quantities, the output interference-to-noise ratio (INR),

$$\text{INR} = \frac{P_i(t')}{P_n(t')} \quad , \quad (60)$$

and the output signal-to-interference-plus-noise ratio (SINR),

$$\text{SINR} = \frac{P_d(t')}{P_i(t') + P_n(t')} \quad , \quad (61)$$

may be computed as functions of  $t'$ .

In the next section, we present an example to illustrate the use of this technique.

### III. AN EXAMPLE

Consider a modulation envelope of the form

$$a_i(t') = \frac{1}{2} (1 + \cos \omega_m' t') \quad . \quad (62)$$

For this  $a_i(t')$ , the interference is an ordinary amplitude modulated signal, as shown in Figure 2, with 100% modulation. The coefficient  $1/2$  in (62) is included to normalize  $a_i(t')$  as in (11). The Fourier coefficients of

$$a_i^2(t') = \frac{1}{4} (1 + \cos \omega_m' t')^2 \quad (63)$$

are

$$p_0 = \frac{3}{8} \quad (64)$$

$$p_{\pm 1} = \frac{1}{4} \quad (65)$$

and

$$p_{\pm 2} = \frac{1}{16} \quad (66)$$

The system in (51) becomes

$$\begin{bmatrix} h_N + p_0 & p_1 & p_2 & 0 & 0 & 0 & \dots & 0 \\ p_{-1} & h_{N-1} + p_0 & p_1 & p_2 & 0 & 0 & \dots & 0 \\ \vdots & \vdots & \vdots & \vdots & \vdots & \vdots & \ddots & \vdots \\ 0 & \dots & p_{-2} & p_{-1} & h_0 + p_0 & p_1 & p_2 & 0 \dots 0 \\ \vdots & \vdots & \vdots & \vdots & \vdots & \vdots & \ddots & \vdots \\ \vdots & \vdots & \vdots & \vdots & \vdots & \vdots & \ddots & \vdots \\ 0 & 0 & \dots & \dots & \dots & 0 & p_{-2} & p_{-1} & h_{-N} + p_0 \end{bmatrix} \begin{bmatrix} \alpha_{N,1} \\ \alpha_{N-1,1} \\ \vdots \\ \alpha_{0,1} \\ \vdots \\ \alpha_{-N,1} \end{bmatrix} = \begin{bmatrix} 0 \\ 0 \\ \vdots \\ C \\ 0 \\ \vdots \\ 0 \end{bmatrix} \quad (67)$$

where  $C$  and  $h_n$  are defined in (48) and (49).

In general, one finds that the number of terms  $N$  needed to construct  $W(t')$  from the series (50) varies with the signal parameters. In each case, one must increase  $N$  until the first four terms on each end of the  $\alpha_{n,1}$  vector in (67) are essentially zero and until the values of  $\alpha_{n,1}$  for small  $n$  are not affected by further increases in  $N$ . To solve (67), we have used Gauss elimination with full pivoting [11,12] and also double precision (16 decimal places on the VAX-11/780). In initial tests of this method, the weight vector  $W(t')$  was checked in numerous cases against Runge-Kutta solutions [11,12] of (1).

As discussed above, time varying weights have two effects on array performance. They cause the array to modulate the desired signal, and they cause the array output signal-to-interference-plus-noise ratio (SINR) to vary periodically with time. In part A below, we show typical curves of desired signal modulation, output INR and SINR as functions of time. In Parts B-E, we describe the effect of each signal parameter on the desired signal modulation. In Part F, we assume the array is used in a digital communication system and describe the effect of this interference on bit error probability.

#### A. Typical Waveforms

Figures 3, 4 and 5 show typical curves of  $a_{dn}(t')$ , output INR and SINR as functions of time over one period of the modulation. These curves are for the case  $\theta_d=0^\circ$ ,  $\theta_i=5^\circ$ ,  $\xi_d=10$  dB,  $\xi_i=20$  dB and

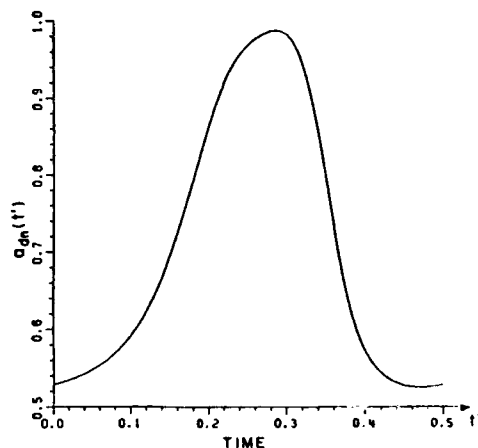


Figure 3.  $A_{dn}(t')$  versus time.  
 $\theta_d=0^\circ$ ,  $\theta_i=5^\circ$ ,  $\xi_d=10$  dB.  
 $\xi_i=20$  dB,  $f'_m=2$ .

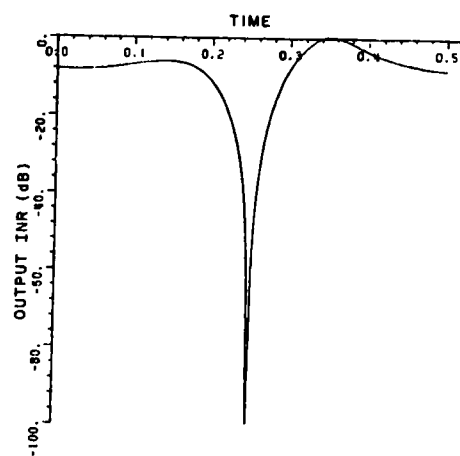


Figure 4. INR versus time.  
 $\theta_d=0^\circ$ ,  $\theta_i=5^\circ$ ,  $\xi_d=10$  dB.  
 $\xi_i=20$  dB,  $f'_m=2$ .

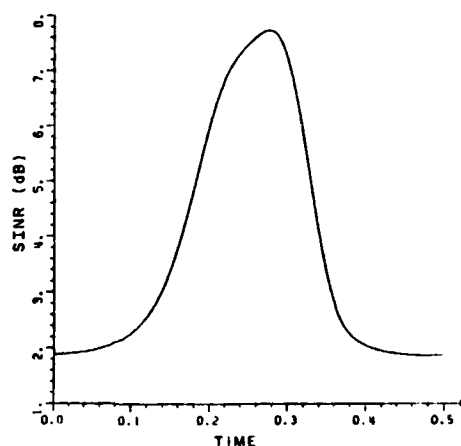


Figure 5. SINR versus time.  
 $\theta_d=0^\circ$ ,  $\theta_i=5^\circ$ ,  $\xi_d=10$  dB.  
 $\xi_i=20$  dB,  $f'_m=2$ .

$f_m' = 2$  (where  $f_m' = \frac{\omega_m}{2\pi}$ ). As may be seen, for this set of parameters, the AM interference signal produces substantial envelope modulation, and the output INR and SINR vary considerably over the modulation period.

Calculations of the phase  $\eta_d(t')$  in (53), on the other hand, show that  $\eta_d(t')$  is constant. The adaptive array does not produce phase modulation on the desired signal with this interference. This important result occurs for all signal parameters, not just those used in Figures 3 through 5. The same result was also found for pulsed interference [2] and for DSBSC-AM interference [3].

Figures 3 through 5 are intended merely to illustrate typical array behavior with AM interference. In general, the desired signal modulation and the SINR variation depend greatly on the choice of signal parameters  $\theta_d$ ,  $\epsilon_d$ ,  $\theta_i$ ,  $\epsilon_i$  and  $f_m'$ . In Parts B-E below, we describe the effect of each signal parameter on the desired signal modulation. To characterize the desired signal modulation, we define three quantities. First, we let  $a_{\max}$  and  $a_{\min}$  be the maximum and minimum values of  $a_{dn}(t')$  during the modulation period. Then we define

$$m = \frac{a_{\max} - a_{\min}}{a_{\max}} \quad (68)$$

$m$  is the fractional modulation on the desired signal. We shall refer to  $a_{\max}$  as the envelope peak and to  $m$  as the envelope variation. In Parts B-E, we describe how  $m$  and  $a_{\max}$  depend on each signal parameter.



### B. The Effect of Angle of Arrival

Desired signal modulation is small unless  $\theta_i$  is close to  $\theta_m$ . When  $\theta_i$  is far from  $\theta_d$ , the envelope variation  $m$  is small and the peak  $a_{\max}$  is close to unity. Figures 6 and 7 show typical curves of  $m$  and  $a_{\max}$  as functions of  $\theta_i$  for the parameters  $\theta_d=0^\circ$ ,  $\xi_d=10$  dB and  $f'_m=2$ . Two curves are shown on each figure, for  $\xi_i=10$  dB and 20 dB.

### C. The Effect of Modulation Frequency

The variation  $m$  and the peak  $a_{\max}$  are large at low  $f'_m$  and drop as  $f'_m$  increases. Figures 8 and 9 show  $m$  and  $a_{\max}$  as functions of  $f'_m$  for the case  $\theta_d=0^\circ$ ,  $\xi_d=0$  dB and  $\xi_i=20$  dB.

### D. The Effect of Interference-to-Noise Ratio

For low  $f'_m$ , the variation  $m$  is largest at high INR. For intermediate values of  $f'_m$ ,  $m$  peaks at intermediate INR.  $a_{\max}$  is unity for low  $f'_m$  and drops to a minimum at high  $f'_m$ . The larger the INR, the farther  $a_{\max}$  drops for large  $f'_m$ . These effects may be seen in Figures 10 and 11, which show  $m$  and  $a_{\max}$  for  $\theta_d=0^\circ$ ,  $\theta_i=5^\circ$ ,  $\xi_d=0$  dB and for five values of  $\xi_i$  between 0 and 30 dB.

### E. The Effect of Desired Signal-to-Noise Ratio

The variation  $m$  is largest and the peak  $a_{\max}$  is smallest for low  $\xi_d$ . As  $\xi_d$  is increased,  $m$  decreases and  $a_{\max}$  increases. Figures 12 and

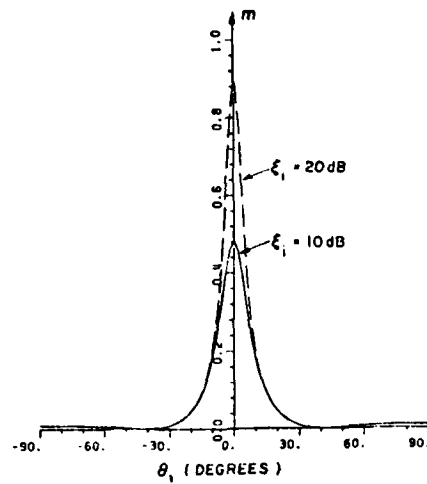


Figure 6.  $m$  versus  $\theta_i$   
 $\theta_d = 0^\circ$ ,  $\xi_d = 10$  dB,  $f'_m = 2$ .

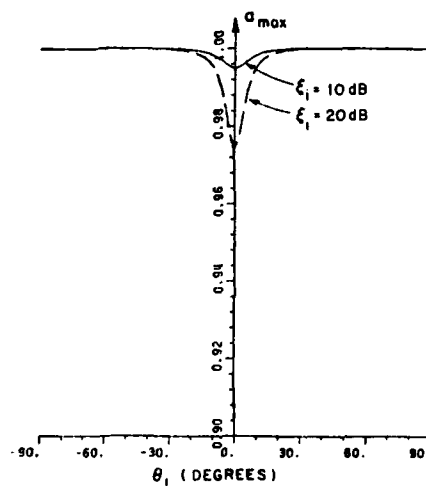


Figure 7.  $a_{\max}$  versus  $\theta_i$   
 $\theta_d = 0^\circ$ ,  $\xi_d = 10$  dB,  $f'_m = 2$ .

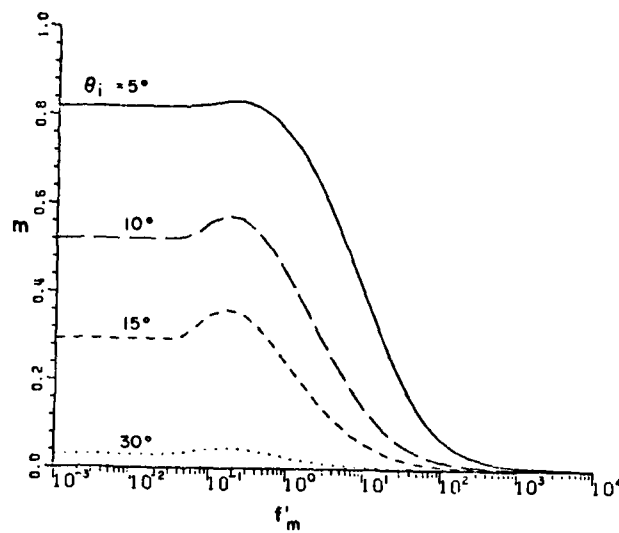


Figure 8.  $m$  versus  $f'_m$   
 $\theta_d = 0^\circ$ ,  $\epsilon_d = 0$  dB,  $\epsilon_i = 20$  dB.

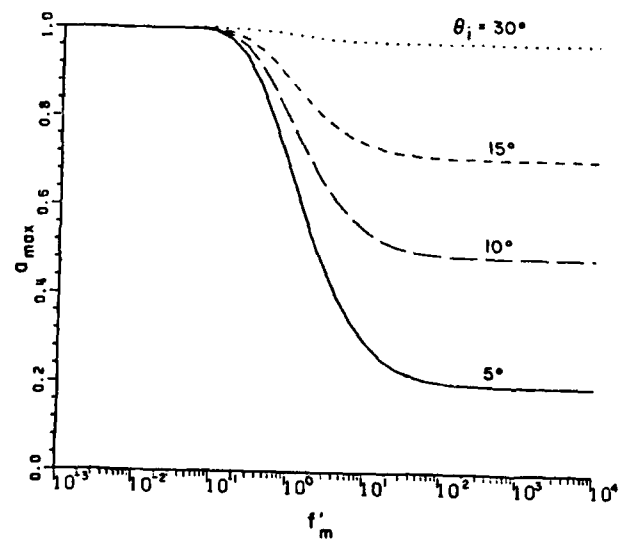


Figure 9.  $a_{\max}$  versus  $f'_m$   
 $\theta_d = 0^\circ$ ,  $\epsilon_d = 0$  dB,  $\epsilon_i = 20$  dB.

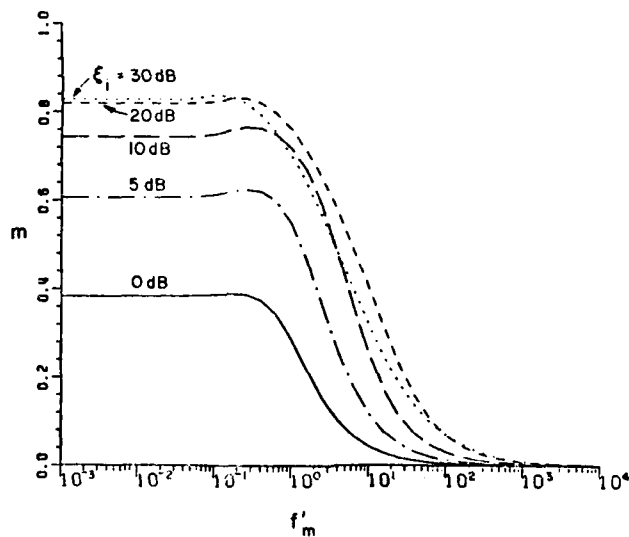


Figure 10.  $m$  versus  $f'_m$   
 $\theta_d = 0^\circ$ ,  $\theta_i = 5^\circ$ ,  $\xi_d = 0$  dB.

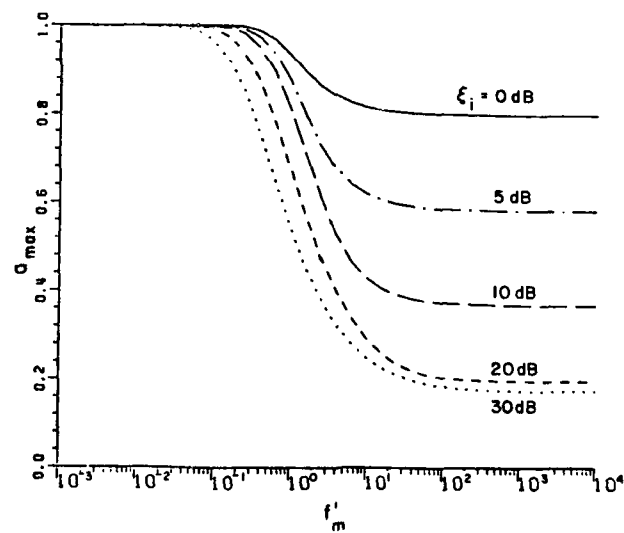


Figure 11.  $a_{\max}$  versus  $f'_m$   
 $\theta_d = 0^\circ$ ,  $\theta_i = 5^\circ$ ,  $\xi_d = 0$  dB.

13 show  $m$  and  $a_{\max}$  for  $\theta_d=0^\circ$ ,  $\theta_i=5^\circ$ ,  $\xi_i=20$  dB and for four values of  $\xi_d$  between 0 and 30 dB. It is seen that for a given  $\xi_d$ ,  $m$  peaks at intermediate values of  $f'_m$ .

#### F. Bit Error Probability

To evaluate the effect of the time-varying SINR, we assume the desired signal is a DPSK biphase modulated signal [13]. We assume the bit rate on the desired signal is much larger than the modulation frequencies in  $a_i(t)$ . As shown in [2,3], under these conditions we may determine the effective bit error probability  $\bar{P}_e$  by averaging the instantaneous bit error probability over one period:

$$\bar{P}_e = f'_m \int_0^{1/f'_m} \frac{1}{2} e^{-\text{SINR}(t')} dt' \quad . \quad (69)$$

Figure 14 shows typical curves of  $\bar{P}_e$  as a function of  $f'_m$  for  $\theta_d=0^\circ$ ,  $\theta_i=30^\circ$ ,  $\xi_d=6$  dB and for several values of  $\xi_i$  between -10 dB and 30 dB. It is seen that the average bit error probability is affected very little by  $f'_m$ . It may be shown that  $\bar{P}_e$  is essentially the same as that for CW interference with an INR of  $(3/8)\xi_i$ , i.e., with the same time-average power as the AM interference signal.

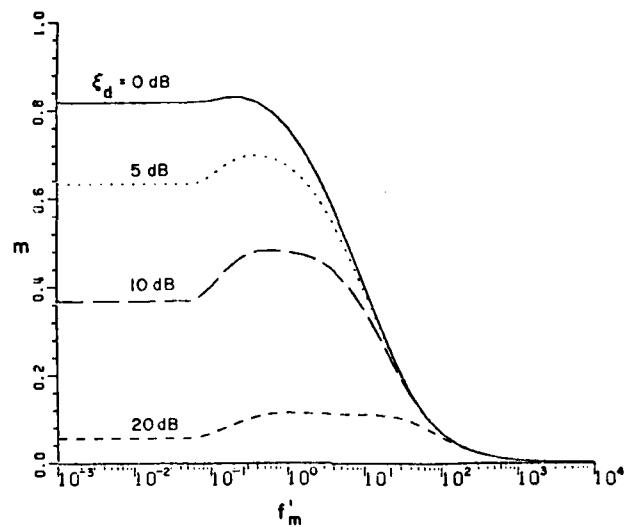


Figure 12.  $m$  versus  $f_m'$   
 $\theta_d = 0^\circ$ ,  $\theta_i = 5^\circ$ ,  $\xi_i = 20$  dB.

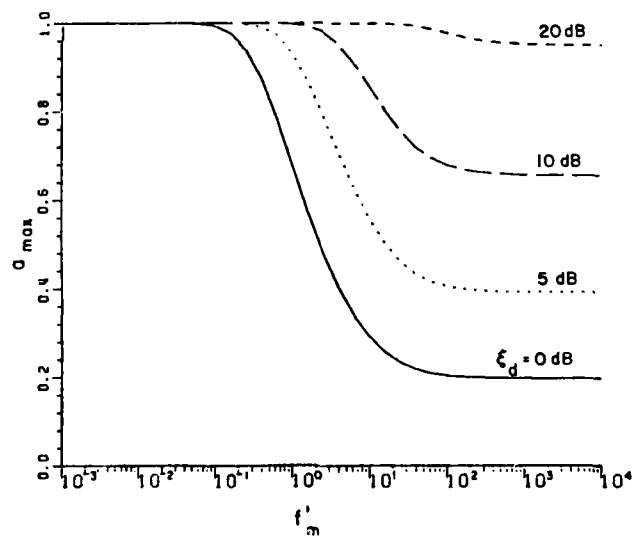


Figure 13.  $a_{\max}$  versus  $f_m'$   
 $\theta_d = 0^\circ$ ,  $\theta_i = 5^\circ$ ,  $\xi_i = 20$  dB.

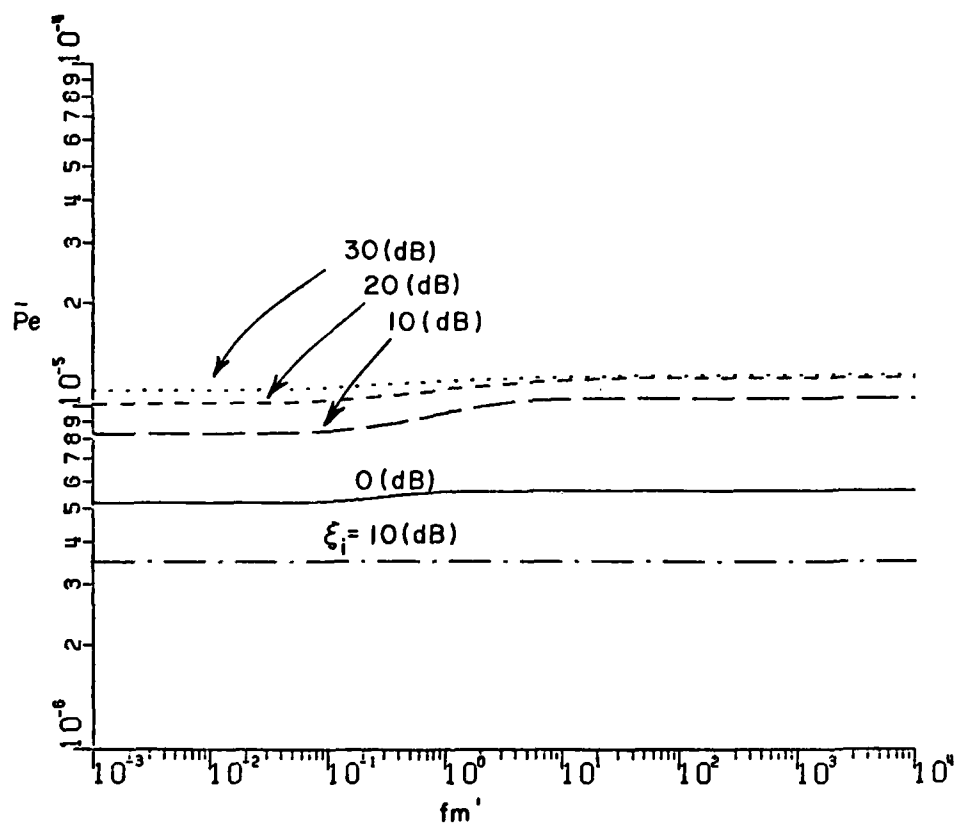


Figure 14. Bit error probability versus  $f_m'$   
 $\theta_d = 0^\circ$ ,  $\theta_i = 30^\circ$ ,  $\xi_d = 6 \text{ dB}$ .

#### IV. SUMMARY

We have developed a mathematical technique for computing the array weights when the array is subjected to interference with periodic envelope modulation. Our approach requires that the envelope modulation be modeled with a finite number of Fourier Series terms.

To illustrate the use of this technique, we have evaluated the effects of an AM interference signal on the array. It was shown that the major effect of AM interference is to cause envelope modulation, but not phase modulation, on the desired signal. The effects of each signal parameter on desired signal modulation have been described. When the desired signal is a DPSK signal, AM interference was found to have essentially the same effect on bit error probability as CW interference. These results are similar to those obtained for DSBSC-AM interference [3].

#### V. REFERENCES

1. B. Widrow, P.E. Mantey, L.J. Griffiths and B.B. Goode, "Adaptive Antenna Systems", Proc. IEEE, Vol. 55, p. 2143, December 1967.
2. R.T. Compton, Jr., "The Effect of a Pulsed Interference Signal on an Adaptive Array", IEEE Trans. Aerospace and Electronic Systems, Vol. AES-18, p. 297, May 1982.
3. A.S. Al-Ruwais and R.T. Compton, Jr., "Adaptive Array Behavior with Sinusoidal Envelope Modulated Interference", accepted for publication in IEEE Transactions on Aerospace and Electronic Systems.



4. P.M. Morse and H. Feshbach, Methods of Theoretical Physics, McGraw-Hill Book Co., New York, 1953; Section 5.2, p. 555ff.
5. R.L. Riegler and R.T. Compton, Jr., "An Adaptive Array for Interference Rejection", Proc. IEEE, Vol. 61, p. 748, June 1973.
6. R.T. Compton, Jr., R.J. Huff, W.G. Swarner and A.A. Ksienski, "Adaptive Arrays for Communication Systems: An Overview of Research at The Ohio State University", IEEE Trans. Antennas Propagation, Vol. AP-24, p. 599, September 1978.
7. R.T. Compton, Jr., "An Adaptive Array in a Spread Spectrum Communication System", Proc. IEEE, Vol. 66, p. 289, March 1978.
8. J.H. Winters, "Spread Spectrum in a Four-Phase Communication System Employing Adaptive Antennas", IEEE Trans. on Communications, Vol. COM-30, p. 929, May 1982.
9. H. D'Angelo, Linear Time-Varying Systems: Analysis and Synthesis, Allyn and Bacon, Boston, 1970.
10. R.S. Kennedy, Fading Dispersive Communication Channels, John Wiley and Sons, New York, 1969.
11. D.M. Young and R.T. Gregory, A Survey of Numerical Mathematics, Addison-Wesley Publishing Co., Reading, Massachusetts, 1972.
12. F.B. Hildebrand, Introduction to Numerical Analysis, McGraw-Hill Book Co., New York, 1974.
13. W.C. Lindsey and M.K. Simon, Telecommunication Systems Engineering, Prentice-Hall Inc., Englewood Cliffs, New Jersey, 1973.

4. P.M. Morse and H. Feshback, Methods of Theoretical Physics, McGraw-Hill Book Co., New York, 1953; Section 5.2, p. 555ff.
5. R.L. Riegler and R.T. Compton, Jr., "An Adaptive Array for Interference Rejection", Proc. IEEE, Vol. 61, p. 748, June 1973.
6. R.T. Compton, Jr., R.J. Huff, W.G. Swarner and A.A. Ksienski, "Adaptive Arrays for Communication Systems: An Overview of Research at The Ohio State University", IEEE Trans. Antennas Propagation, Vol. AP-24, p. 599, September 1978.
7. R.T. Compton, Jr., "An Adaptive Array in a Spread Spectrum Communication System", Proc. IEEE, Vol. 66, p. 289, March 1978.
8. J.H. Winters, "Spread Spectrum in a Four-Phase Communication System Employing Adaptive Antennas", IEEE Trans. on Communications, Vol. COM-30, p. 929, May 1982.
9. H. D'Angelo, Linear Time-Varying Systems: Analysis and Synthesis, Allyn and Bacon, Boston, 1970.
10. R.S. Kennedy, Fading Dispersive Communication Channels, John Wiley and Sons, New York, 1969.
11. D.M. Young and R.T. Gregory, A Survey of Numerical Mathematics, Addison-Wesley Publishing Co., Reading, Massachusetts, 1972.
12. F.B. Hildebrand, Introduction to Numerical Analysis, McGraw-Hill Book Co., New York, 1974.
13. W.C. Lindsey and M.K. Simon, Telecommunication Systems Engineering, Prentice-Hall Inc., Englewood Cliffs, New Jersey, 1973.

**END**

**FILMED**

**5-83**

**DTIC**